International Journal of Mechanical and Production Engineering Research and Development (IJMPERD)
ISSN (P): 2249-6890; ISSN (E): 2249-8001
Vol. 8, Issue 2, Apr 2018, 637-648

DESIGN AND ANALYSIS OF MICRO AIR VEHICLE WITH ZIMMERMAN PLATFORM

GELLA SHIVA DURGA MADHAV[1], YELLURI SHWETHA[2] & DUSSA GOVARDHAN[3]

[1,2]*Assistant Professor Institute of Aeronautical Engineering, Dundigal, Hyderabad, India*

[3]*Professor Institute of Aeronautical Engineering, Dundigal, Hyderabad, India*

ABSTRACT

A Micro air vehicle of span 0.15 meter as basic prerequisite is designed with Zimmerman wing such that the structure is small enough, promised with high structural integrity and to serve its function for optical surveillance with all different electronic components used in the successful MAVs. Zimmerman wing which has a distinct characteristic of low aspect ratio and low Reynolds number is designed by considering several conceptual design stages. The weight estimation was done including specified electronic components. Lift and Drag forces are evaluated for different AOA and at different velocities through computational analysis for this design. The final design results show that the design can fly at certain operating conditions.

KEYWORDS: Zimmerman Wing, Successful MAVs & Different AOA

Received: Jan 24, 2018; **Accepted**: Feb 14, 2018; **Published**: Mar 12, 2018; **Paper Id:** IJMPERDAPR201875

Original Article

INTRODUCTION

The increasing demand for miniature-sized vehicles which can perform the surveillance operations more efficiently in an undetectable manner was the major driving factor behind the development of the MAVs though they are being used for different purposes today[x]. As the technology progressed, there is a need for further reduction in the size of the vehicle so that it remains unidentified while performing the given task. The small size of the vehicle imposes constraints on the weight of the structure and on the payload that can be carried on the vehicle[x]. The strength to weight ratio plays an important role in the fabrication of the vehicle. The structural integrity of the MAV has to be maintained for its proper functioning. Wings of AR less than 1.25 depicted abnormally high coefficients of lift[x] (higher than those obtainable even with infinite wings) and correspondingly high angles of attack. The semicircular wing tip models (Zimmerman) exhibits superior performance compared to the other shapes[x]. This semicircular wing tip model is known as Zimmerman. Wing geometry is one of the important parameters which affect the aerodynamic characteristics of Low Aspect Ratio wings at low Reynolds numbers[x]. The Zimmerman was chosen for its distinct geometric characteristics. The advantage of this shape is the lower interference of the tip vortices on the top of the planform due to its semicircular shape[x]. The Zimmerman and inverse Zimmerman plan-forms are based on wingtip shapes designed by Zimmerman in the 1930s. It consists of two half ellipses joined either at the quarter chord location (in case of Zimmerman planform) or at the three quarter chord location (in case of the inverse Zimmerman planform). One ellipse has semi-major axis a3 and semi-minor axis $a_{1,}$ while the other has semi-major axis a_2 and semi-minor axis a_3[x]. Similar is the formation of inverse Zimmerman plan form. Wing plan forms were found to have significant aerodynamic effects on the lift and drag

coefficients and results for the lift coefficients showed large non-line arities for aspect ratios below 1.25[x]. The Reynolds Number had a small effect on the performance of LAR wings for the range of Re of 100,000 to 200,000[x]. The effect of wing plan form on the lift characteristics of LAR wings for a given aspect ratio and Reynolds number can be further analyzed by introducing the parameter $x_{max\ span.}$ $x_{max\ span}$ is the chord wise location (measured from leading edge) of maximum wingspan, non-dimensionalised by the root chord of the model[x]. For the Zimmerman, elliptical and inverse Zimmerman wings, $x_{max\ span}$ is 0.25, 0.5 and 0.75 respectively. For the rectangular wings, $x_{max\ span}$ is taken to be 1.0 rather than 0[x].

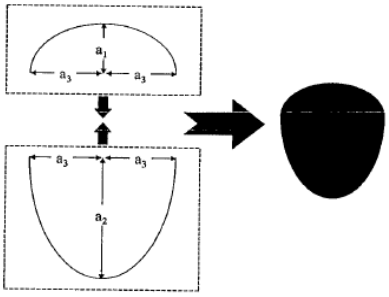

Figure 1: Planform of Zimmerman

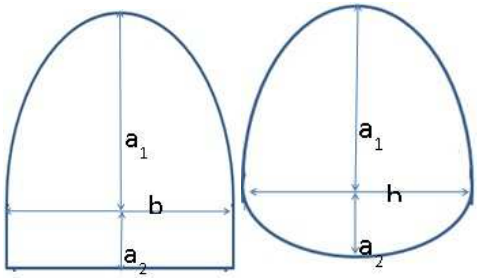

Figure 2: Planform of Inverse Zimmerman

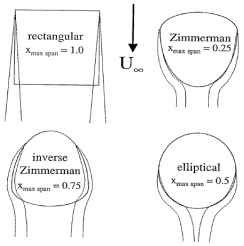

Figure 3: Different Planforms of Zimmerman

For wing shapes in which the maximum span is located upstream of the half-root-chord location ($x_{max\ span} < 0.5$), the tip vortices are seen to first develop at the location of the maximum wingspan. The vortices then follow the outline of the wing up to a point and separate from the wing. In contrast, for wings with $x_{max\ span}$ greater than 0.5, the vortices are seen to separate from the wing location of maximum span[x]. Thus the vortices of wings with $x_{max\ span} > 0.5$ are further apart than those of wings with $x_{max\ span} < 0.5$[x]. One direct way to measure lift performance is to compare the lift-curve slope, $C_{L\alpha,}$ for each wing and aspect ratio[x].

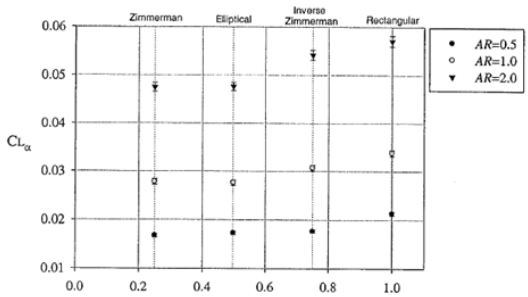

Figure 4: Lift-Curve Slope for Different Planforms of Zimmerman

CONCEPTUAL DESIGN

Aerofil Selection

The shape of airfoil is an important feature for the flying wing along with the planform shape. Among all the low Reynolds number airfoils the following four were considered CLARK-Y, FX 60-100, E 193 and S5020 are taken into consideration[x]. The design lift co-efficient values were calculated as follows

For straight and level flight, we have[x]

$$C_L = \frac{W}{(1/2)\rho v_\infty^2 S} \quad (1)$$

By considering the above-derived values

Estimated weight (W): 1.0094 N $a_1 = 0.75\ C_{root} = 0.0954$ m

Density(ρ): 1.225 Kg/m^3 $a_2 = 0.25 C_{root} = 0.0317$ m

Velocity (V): 10 m/s

Area (S): 0.0160 m^2

$C_L = 103/V^2$

And accounting that the velocity in the low Reynolds number region varies from 10 m/s to15 m/s we have

Table 1: C_L Values at Different Velocities

V(m/s)	C_L
10	1.0300
11	0.8342
12	0.7009
13	0.5972
14	0.5150
15	0.4486

The C_L of the aerofoil is close to that of the wing[x]. Hence in choosing the aerofoil we rely on the C_L values obtained for aerofoil. As the plan for shape is modified the effective or reference area, this planform is increased. Retaining the span of 0.15 m, area increases to 0.0160 m^2 & the Aspect Ratio changes to 1.3. The results obtained from the software at10 m/s are as follows

Data inferred from software (at 10 m/s)

Table 2

AIRFOIL	CLARK-Y	FX 60-100	E 193	S5020
Required lift coefficient	1.030	1.030	1.030	1.030
Maximum lift coefficient	1.003	1.126	0.957	0.788
Thickness (%)	11.7	10	10.2	8.4
Camber (%)	3.6	3.5	3.6	2.6
Leading edge radius (%)	1.8	1.2	1.9	1.7

Among the four mentioned aerofoils, only FX 60-100 gives maximum lift coefficient greater than the required lift coefficient that leaves behind all other aerofoils. Even in the leading edge radius point of view, it has the lowest leading edge radius that complies with the criterion. Although S5020 has a lowest thickness ratio the compromising factor is lift

coefficient which is given by merely FX 60-100. Hence we selected **FX 60-100** aerofoil for design of MAV.

For FX 60-100 we have the following result[x]

FX60-100 10.0% smoothed

Angle of Zero Lift: -4.566 Degrees
Aerodynamic Center: x/c= 0.2484 y/c= 0.0001
Pitch Coefficient about the Aerodynamic Center: -0.122

Reynolds Number: 74,786

Alpha	Lift Coef	Pitch Coef	Drag Coef	L/D Ratio	Lower Surface Turb	Lower Surface Sep	Upper Surface Turb	Upper Surface Sep
-2.00	0.278	-0.123	0.0142	19.6	0.3179	1.0000	0.7039	0.9931
-0.50	0.441	-0.123	0.0145	30.4	0.3620	1.0000	0.6442	0.9923
1.00	0.604	-0.123	0.0152	39.8	0.4069	1.0000	0.5623	0.9923
2.50	0.768	-0.123	0.0166	46.3	0.4860	1.0000	0.4169	0.9932
4.00	0.917	-0.123	0.0181	50.6	0.5863	1.0000	0.3539	0.9856
5.50	1.044	-0.123	0.0223	46.8	1.0000	1.0000	0.0695	0.9680
7.00	1.126	-0.125	0.0258	43.7	1.0000	1.0000	0.0378	0.9315
8.50	1.074	-0.130	0.0302	35.6	1.0000	1.0000	0.0227	0.8408
10.00	-0.639	-0.181	0.0297	-21.5	1.0000	1.0000	0.0022	0.0512

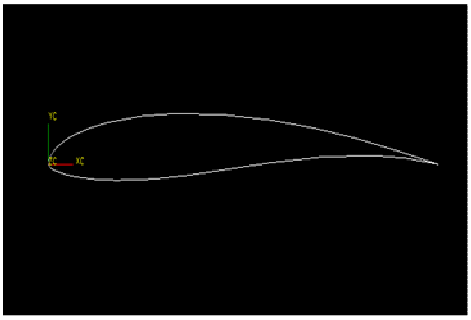

Figure 5: Airfoil Geometry

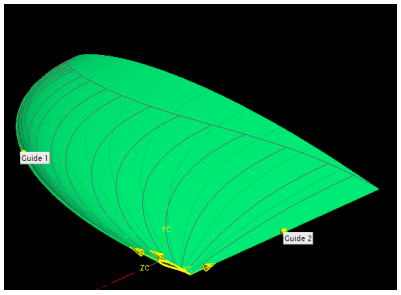

Figure 6: Generation of Zimmerman for Selected Airfoil

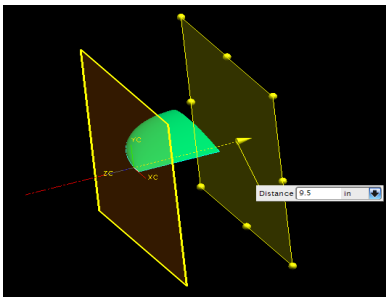

Figure 7

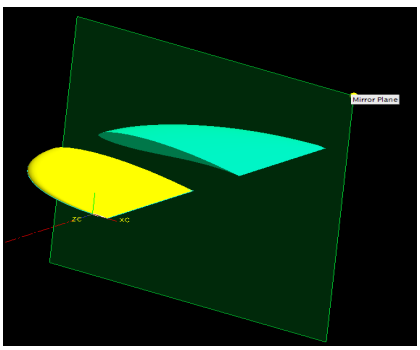

Figure 8: Generation of Zimmerman for Selected Airfoil

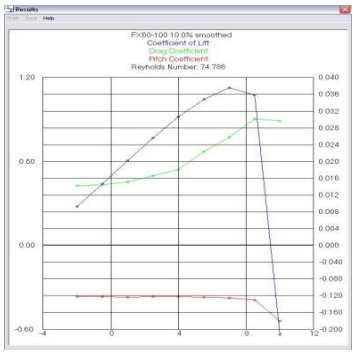

Figure 9

Sizing of Elevons and Rudder

Mean Aerodynamic Chord (MAC) = $\frac{2b\ Croot^2}{3S}$ = 109.8 mm(Abbott, I.H., and Von Doenhoff, A.E. (1959), *Theory of Wing Sections*, Section 1.4 (page 27), Dover Publications Inc., New York, Standard Book Number 486-60586-8)

Prior to sizing of the rudder the vertical tail geometry should be determined. The tail aspect ratio is assumed to be 1.5. The tail chord length is assumed to be 45% of the mean aerodynamic chord of the wing and the geometrical shape as triangular.

C_t = 50 mm

Aspect Ratio (AR) = 1.5

Tail Area (S_t) = $(0.5C_t \times b_t)$

AR = $\frac{b_t^2}{S_t}$

The Rudder is assumed to be 30% of the tail chord length[x] as said by Daniel Raymer.

Chord length of rudder 112.5 mm

The Rudder is assumed to be 30% of the tail chord length.

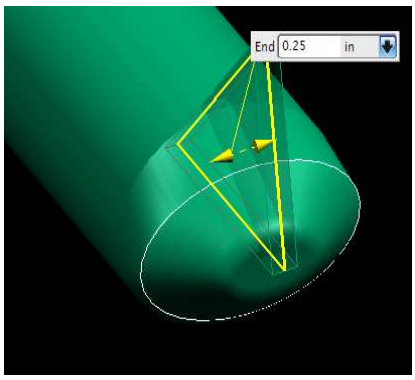

Figure 10: Geometry of Control Surface on Fuselage

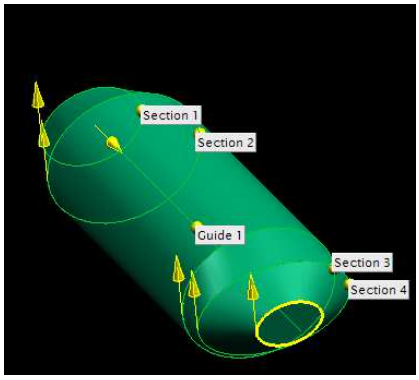

Figure 11: Geometry of Fuselage

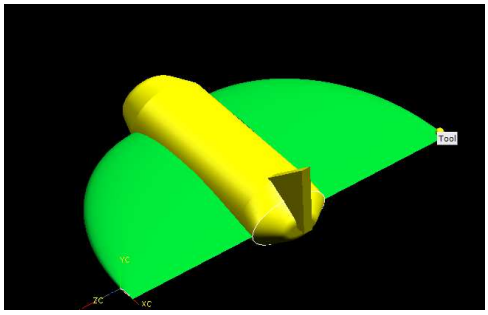

Figure 12: Geometry of Complete MAV

Weight Estimation

Above requirements encompasses Motor, Battery, GPS System, Camera, Vehicle Structure, Servo motors, Payload and miscellaneous parts. For the MAV design initial estimation of each of the part with its upper and lower limit

of weight is necessary. These figured requisites should be chosen such that it complies with the outlined size of the MAV with as lowest weight as possible. After the Estimation is made best quality product which best suits the design and serve the purpose is chosen finally.

The following table gives the estimated weights for respected requisites:

Table 3

Component	Estimated Weight (grams)
Motor	8-15
Battery	20-35
GPS	30-45
Camera	1-5
Vehicle Structure	15-25
Servo motor	4-8
Miscellaneous	5
Total	**83-138**

Final components selected are given in the table

Table 4

Component	Name
Motor	Wes Technik micro MNC-524
Electronic speed controller	Phoenix-10
Battery	Kokam slpb433452
Servos	Wes-Technik ls-2.0
Camera	Kx-1 micro color CMOS
Autopilot	3520 MAVAuto Pilot

The 3520 MAV auto pilot is selected and it has inbuilt GPS receiver and all the relevant ports to support servo motors, batteries, and camera. As this device would reduce the weight of individual receivers for each system this component is selected.

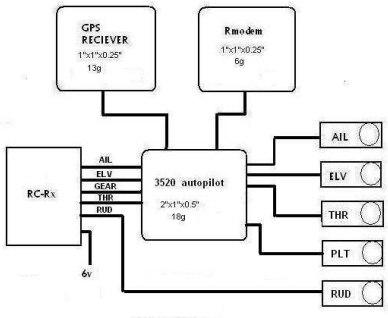

Figure 13: Block Diagram of Autopilot

Aerodynamic Analysis

The complete CFD analysis is carried in ANSYS CFX Fluent software with following Boundary conditions.

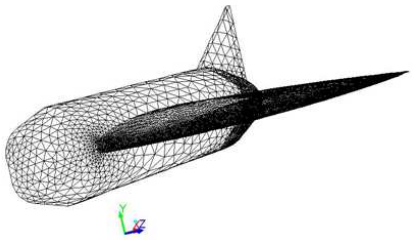

Figure 14

Table 5: Boundary Conditions

Name	Boundary Type	Value
Velocity Inlet	Velocity _inlet	15 m/s (Magnitude)
Outlet	Pressure _Outlet	0 (Gauge Pressure)
Airplane Surface	Wall	-
Walls	Wall	-
Symmetric surface	Symmetry	-
Fluid Flow	Fluid	-

Table 6: Solution Methods

Scheme	Simple
Gradient	Green - Gauss Cell Based
Pressure	Standard
Momentum	First Order Momentum
Modified Turbulent Viscosity	First Order Momentum

Similar procedure is followed for analysis at other velocities. Results for velocities 10 m/s -14 m/s

RESULTS AND DISCUSSIONS

Various Contours like Static Pressure, Pressure Coefficient, Total Pressure, Velocity Magnitude, turbulence viscosity contours are plotted to analyze the behaviour of MAV. Pressure coefficient plots are plotted to observe its variations along the surface of MAV. Lift and Drag forces along with their coefficients are obtained at different angle of attacks.

At velocity=10 m/s

Table 7

Angle of Attack	Lift Force	Drag Force	Coefficient of Lift	Coefficient of Drag
0	0.56410458	0.18619676	0.5756169184	0.1899966939
5	0.56410458	0.23342104	0.5756169184	0.2381847347
10	0.57394618	0.27886577	0.585659363	0.2845569082
15	0.57942055	0.3221913	0.5912454592	0.3287666327
17	0.58037691	0.33885565	0.5922213265	0.3457710714
18	0.58058982	0.34703135	0.5924385918	0.3541136224
19	0.58062612	0.35507667	0.5924756327	0.5924756327
20	0.58048514	0.36306834	0.5923317755	0.5923317755

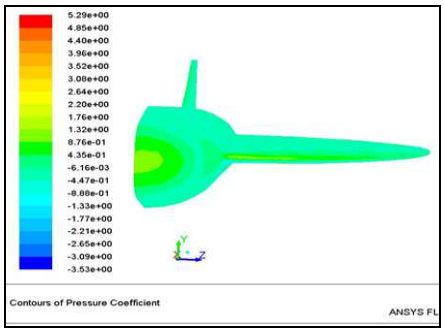

Figure 15: Variation of Pressure Co-Efficient and Static Pressure on MAV

At velocity=11 m/s

Table 8

Angle of Attack	Lift Force	Drag Force	Coefficient of Lift	Coefficient of Drag
0	0.66468796	0.22260609	0.5605396863	0.1877265053
5	0.68155996	0.27969017	0.5747680553	0.2358662253
10	0.69324431	0.33464192	0.5846216057	0.2822077247
15	0.69965365	0.38705065	0.5900266908	0.3264046635
17	0.70072795	0.40721441	0.5909326615	0.3434090150
18	0.70094485	0.41710823	0.5911155761	0.3517525974
19	0.70094863	0.42720124	0.5911187631	0.3602641592
20	0.70073813	0.43651801	0.5909412464	0.3681211081

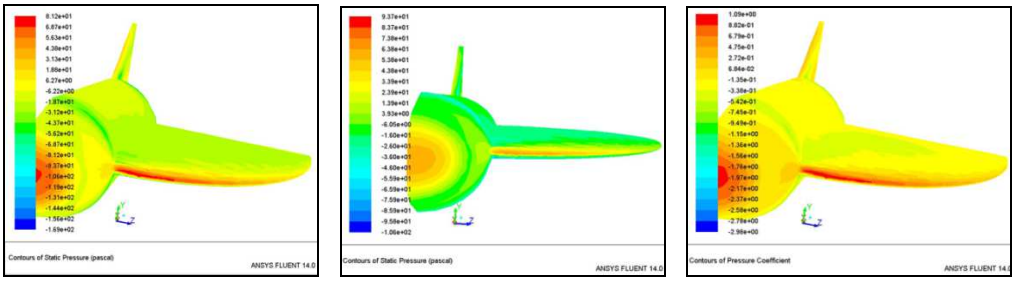

Figure 16: Variation of Pressure Co-Efficient and Static Pressure on MAV

At velocity= 14 m/s

Table 9

Angle of Attack	Lift Force	Drag Force	Coefficient of LIft	Coefficient of Drag
0	1.0629583	0.35348985	0.5533935339	0.1840326166
5	1.0897220	0.44478701	0.5673271554	0.2315634163
10	1.1081914	0.53269313	0.5769426281	0.2773287849
15	1.1182278	0.61655121	0.5821677426	0.3209866774
17	1.1198625	0.64882070	0.5830187943	0.3377867035
18	1.1201678	0.66465580	0.5831782070	0.3460307164
19	1.1201326	0.68024065	0.5831594127	0.3541444450
20	1.1197547	0.69572389	0.5829626718	0.3622052738

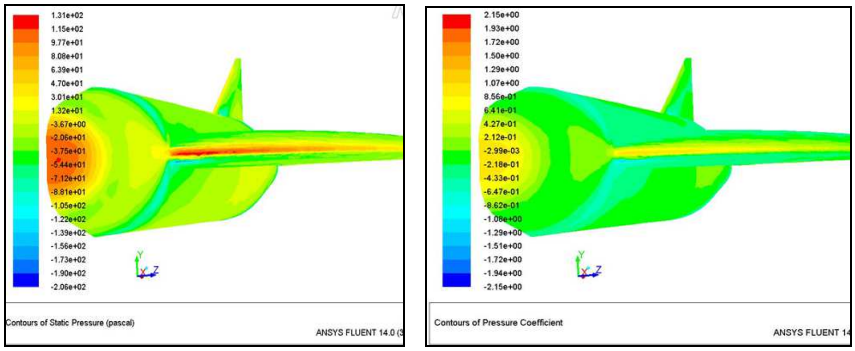

Figure 17:Variation of Pressure Co-Efficient and Static Pressure on MAV

At velocity=15 m/s

Table 10

Angle of Attack	Lift Force	Drag Force	Coefficient of Lift	Coefficient of Drag
0	1.2314910	0.39997296	0.5584993197	0.1813936327
5	1.2161664	0.50578207	0.5515493878	0.2293796236
10	1.2822353	0.60773499	0.5815126077	0.2756167755
15	1.2930492	0.70506971	0.5864168707	0.3197595057
17	1.2946215	0.74254770	0.5871299320	0.3367563265
18	1.2948161	0.76094370	0.5872181859	0.3450991837
19	1.2946176	0.77905238	0.5871281638	0.3533117370
20	1.2940219	0.79704648	0.5868580045	0.3614723265

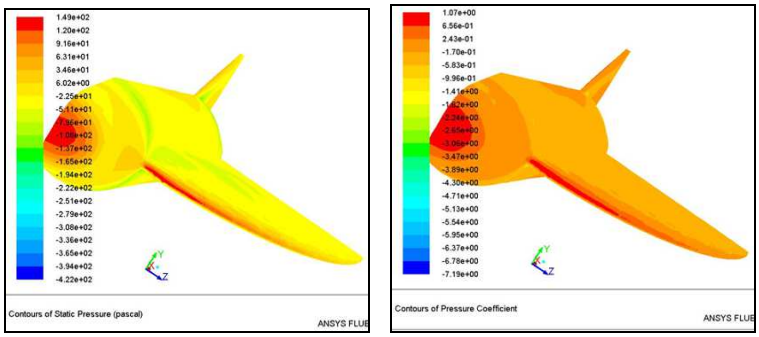

Figure 18: Variation of Pressure Co-Efficient and Static Pressure on MAV

CONCLUSIONS

The aim of this study is to select the best airfoil for MAV. A appropriate initial guess value is taken from the available angle of attacks such that polar graphs are calculated.

This paper has presented a viscous analysis method suitable for incompressible and low Reynolds number airfoils. The Realizable k- ε solution is being used for analysis that helps to converge our results. This analysis needs further investigation with experimental setup for the validation of results to give better estimate of aerodynamics characteristics, especially the effect of closing wing tip and it may influence the aerodynamic performance.

This analysis successfully captured the essential aerodynamics characteristics for the better understanding the aerodynamic performance in conceptual design of MAV

REFERENCES

1. *Davis, W. R., Kosicki, B. B., Boroson, D. M., and Kostishack, D. F, "Micro air vehicles for optical surveillance", The Lincoln Laboratory Journal, Vol. 9, No. 2, 1996, pp. 197-214.*
2. *Galinski, C., and Zbikowski, R. "Some problems of micro air vehicles development", Bulletin of the Polish Academy of Sciences Technical Sciences, Vol. 55, No. 1, 2007, pp. 91-98.*
3. *Hassanalian, M., Khaki, H., Khosrawi, M., "A new method for design of fixed wing micro air vehicle", Proceedings of the Institution of Mechanical Engineers, Journal of Aerospace Engineering, Vol. 229, 2014, pp. 837-850.*
4. *Richardson, T., "Micro UAVs", The Institution of Engineering and Technology Seminar, University of Bristol, 20th February 2007.*
5. *Klingebiel, K. R., "Computational aerodynamics of flapping flight using an indicial response method", M.Sc. Dissertation, Aerospace Engineering Dept. Pennsylvania State University, 2006.*
6. *6Mueller, T. j., "Aerodynamic Measurements at Low Reynolds Numbers for Fixed Wing Micro-Air Vehicles", Hessert Center for Aerospace Research, University of Notre Dame, 1999.*
7. *Chen, Z., "Micro air vehicle design for aerodynamic performance and flight stability", Doctoral dissertation, Mechanical Engineering Dept, University of Sheffield, 2014.*
8. *Turan, M., Canfield, R. A., and Harmon, F. G., "Tools for the conceptual design and engineering analysis of micro air vehicles", 47th AIAA Aerospace Sciences Meeting including The New Horizons Forum and Aerospace,Orlando, Florida, 5-8 Jaunuary.*
9. *Torres, G. E., & Mueller, T. J., "Low aspect ratio aerodynamics at low Reynolds numbers", AIAA journal, Vol. 42, No. 5, 2004, pp. 865-873.*
10. *Marek, P. L., "Design, optimization and flight testing of a micro air vehicle" Doctoral dissertation, University of Glasgow, 2008.*
11. *Flake, J., Frischknecht, B., Hansen, S., Knoebel, N., Ostler, J., &Tuley, B., "Development of the Stableyes Unmanned Air Vehicle", 8th International Micro Air Vehicle Competition, The University of Arizona, Tucson, AZ, 2004, pp. 1-10.*
12. *Zhi-Ping Lin et al.,, Study of Smart Electric Vehicle Charging Path System, International Journal of Computer Networking, Wireless and Mobile Communications (IJCNWMC), Volume 6, Issue 5, September - October 2016, pp. 49-58*
13. *Stanford, B., Sytsma, M., Albertani, R., Viieru, D., Shyy, W., and Ifju, P., "Static Aeroelastic Model Validation of Membrane Micro Air Vehicle Wings", AIAA Journal, Vol. 45, No. 12, 2007, pp. 2828-2837.*
14. *Dornheim, M., A., "Small Drones Mature", Aviation Week and Space Technology, Vol. 159, No. 11, 2003, pp. 63-64.*
15. *Cosyn, P., and Vierendeels, J., "Design of fixed wing micro air vehicles", The Aeronautical Journal, Vol. 111, No. 1119, 2007, pp. 315-326. Downloaded by VIRGINIA TECH on January 11, 2016 | http://arc.aiaa.org | DOI: 10.2514/6.2016-1743 American Institute of Aeronautics and Astronautics 10*
16. *Kellogg, J., Bovais, C., Foch, R., McFarlane, H., Sullivan, and et al., "The NRL Micro Tactical Expendable (MITE) AirVehicle", The Aeronautical Journal of the Royal Aeronautical Society, Vol. 106, No. 1062, 2002, pp. 431-441.*
17. *Mueller, T. J., Kellogg, J. C., Ifju, P. G., and Shkarayev, S. V., "Introduction to the Design of Fixed-Wing Micro Air Vehicles including three case studies", AIAA, Virginia, USA, 2006, pp. 116-117.*
18. *Morris, S. J., "Design and flight test results for micro-sized fixed-wing and VTOL aircraft". In Proceedings of the First*

International Conference on Emerging Technologies for Micro Air Vehicles, Georgia Institute of Technology, Atlanta, GA, February 1997.

19. *Shkarayev, S., Moschetta, J., and Bataille, B., "Aerodynamic design of VTOL micro air vehicles", In Proc. of the MAV07 International Conference, France, September 2007.*
20. *Albertani, R., Boria, F., Bowman, S., Claxton, D., Ifju, P., Johnson, B., and Sytsma, M., "The University of Florida Autonomous Micro Air Vehicle", International Micro Air Vehicle Competition, 2005.*
21. *Zimmerman, C. H., "Aerodynamic characteristics of several airfoils of low aspect ratio", National Advisory Committee for Aeronautics, No. 539, 1935.*
22. *Mueller, T. J., and Torres, G. E., "Aerodynamics of Low Aspect Ratio Wings at Low Reynolds Numbers with Applications to Micro Air Vehicle Design and Optimization", Naval Research Laboratory final report, N00173-98-C2025, USA, Nov. 2001.*